CLOUD COVER DETERMINATION IN POLAR REGIONS FROM SATELLITE IMAGERY

R.G. Barry, J. Key, and J.A. Maslanik

Cooperative Institute for Research in Environmental Sciences
and
Department of Geography
University of Colorado, Boulder

Semi-Annual Report
to
NASA Climate Program

Grant: NAG-5-898

15 December 1988

1.0 Introduction

The principal objectives of this project are

1) to develop suitable validation data sets to evaluate the effectiveness of the International Satellite Cloud Climatology Project (ISCCP) operational algorithm for cloud retrieval in polar regions and to validate model simulations of polar cloud cover;

2) to identify limitations of current procedures for varying atmospheric surface conditions, and to explore potential means to remedy them using textural classifiers; and

3) to compare synoptic cloud data from a control run experiment of the GISS climate model II with typical observed synoptic cloud patterns.

In the first six months of the first project year a methodology was developed for combining AVHRR and SMMR data. These data were calibrated and registered to a polar sterographic projection for subsequent digital analysis (Maslanik et al., in press). Cloud cover and surface types were manually interpreted, viewing angle effects were examined, and the development of a catalog of spectral and textural properties of polar clouds and surfaces was begun. Additionally, cloud analysis and clustering methods such as Coakley and Bretherton's spatial coherence and the fuzzy sets approach were implemented (Key et al., in press).

In the second half of the first year, work continued on the catalog of spectral and textural features, where new combinations of the calibrated AVHRR data (i.e. ratios and differences of AVHRR channels) were included in the analysis and data from two seven-day sequences of imagery for two areas of the Arctic were studied. The spatial coherence method was extended to include time

("temporal coherence") and space and time ("spatiotemporal coherence"). These methods were examined to gain further insight into the spatial and temporal features of polar clouds and surfaces as they effect the functionality of the ISCCP algorithm. Also in the first year, the relationship between theoretical and empirical approaches was examined with the GISS general circulation model, where the spatial and temporal distributions of monthly average cloud fraction were compared to observed cloud amounts.

This report details the current investigations underway and summarizes the progress made to date since the last semi-annual report. The focus has been on the implementation and testing of the basic ISCCP cloud detection algorithm for use with polar data.

2.0 ISCCP

The ISCCP, a project to map clouds with satellite data, began its operational activities in July 1983. ISCCP will provide a uniform global climatology of the satellite-measured radiances and derive an experimental climatology of cloud radiative properties from these radiances. Leading to the development of the ISCCP algorithm, Rossow et al. (1985) compared six cloud algorithms. The results showed that the performance of all algorithms depends on how accurately the clear sky radiances are specified. The ISCCP algorithm now being developed is composed of a series of steps, each of which is designed to detect some of the clouds present in the scene. The current state of the project is such that there is no single version of the algorithm which can be applied to all areas of the globe. The algorithm is currently operational for low latitude data, but performs rather poorly at high latitudes (Rossow, 1987). For this reason, the structure of the ISCCP algorithm is maintained in the cloud

analysis procedure presented here, and much of the research described in the following chapters is aimed at the modification and calibration of the algorithm for use with polar data. At the time of this writing, global results of the ISCCP algorithm are available (as the Pilot Climate Data System C1 data set) for only July, 1983.

The cloud detection procedure of the ISCCP cloud algorithm was applied to satellite observations of the polar regions by Rossow (1987). It was found that the method in general detected too much cloudiness, in part because the algorithm does not distinguish between open water/sea ice and snow-covered/snow-free land, and because thresholds were not "tuned" for the small temperature differences and generally low IR radiances common in the polar regions. No further work on the ISCCP algorithm applied to polar data has been reported in the literature.

2.1 Images Used in Analyses

In order to adapt the ISCCP algorithm for use with polar data, three areas of the Arctic were examined (Figure 1). Study area 1 is centered on the Kara and Barents Sea extending north to the pole and south to Norway and the Siberian coast. Study area 2 covers most of the Canadian Archipelago and Greenland, and extends north to the pole. Study area 3 extends from the coast of Norway to Ellesmere Island. Summer and winter images are available for each location. A seven-day summer series (July 1-7, 1984) of areas 1 and 2, and a winter series (January 6-12, 1984) of area 3 were examined.

While these areas cover only one-third of the Arctic Basin, they include representative samples of all surface types found in the Arctic: snow-covered and snow-free land, sea ice of varying concentrations, open water, and permanent ice cap. In fact, these areas present particularly difficult conditions for

cloud algorithms during the July period; sea ice is moving, snow is melting and ponds form, and the extensive coastlines exhibit mixed temperature regimes. Reflectances in the study areas were found to vary significantly over the short time period and temperatures gradients from North to South were observed.

These conditions are usual for summer in the Arctic, as are the pressure patterns which occurred. Surface pressure maps constructed from Arctic Ocean buoy data provide an overall synoptic picture of daily weather. Serreze and Barry (1988) found that cyclones are uncommon in the eastern portion of the Canadian Archipelago in the summer, but both cyclones and anticyclones are common in and around the Barents Sea. Similar conditions can be seen in the data, so that this time period may be considered as exhibiting "typical" Arctic summer conditions. Although correlations have been determined between synoptic pressure systems, cloud amount, and cloud type (Barry et al., 1987), detailed cloud climatologies for the Arctic are not available and it is therefore more difficult to make such a statement concerning cloud cover. Conditions during the January study period are also similar to the mean pattern and are considered to be typical.

2.2 The ISCCP Algorithm Description

All cloud algorithms consist of two basic steps: cloud detection and cloud analysis. The first step partitions the observed radiances into those representing clouds and those that are clear. In the second step, the quantitative determination of cloud properties is made from the measured radiances. This may involve simply counting cloudy image pixels to obtain a single cloud parameter such as fractional cloud cover, or the process may utilize radiative transfer models to obtain a parameterized set of cloud properties. The ISCCP cloud algorithm has three major components: cloud detection,

radiative analysis, and statistical analysis (Rossow et al., 1985; Rossow, 1987). Of primary concern here is the cloud detection step, with limited attention being devoted to radiative analysis. The algorithm assumptions are that cloud scene radiances are more variable in time and space than clear scene radiances and cloudy scenes are associated with larger visible channel and smaller infrared radiances than clear scenes. Of particular interest in the cloud detection phase is the importance of spatial and temporal variability. The major steps of the basic algorithm are summarized in Figure 2 and are:

Spatial variation. The image is divided into cloudy and clear categories based on cold and warm pixels. If a pixel is much colder than the warmest pixel in a small region ((100 km)^2 over land and (300 km)^2 over ocean), it is label as "cloud". Otherwise, it is labeled "undecided". High and middle level clouds are identified. Only thermal data are used in this step.

Temporal variation. Pixels are compared to the day before and after for changes in temperature. If the middle day is much colder than either the day before or the day after, is it is labeled "cloud". If the variation is small, it is labeled "clear". Those pixels exhibiting intermediate variability are labeled "undecided". Again, only thermal data are used in this step. High and middle clouds are most easily recognized. The class of a pixel based on these two steps is given in the following truth table:

	Temporal Variation		
Spatial Variation	Cloud	Undecided	Clear
Cloud	Cloud	Cloud	Mixed
Undecided	Cloud	Undecided	Clear

Compositing. The mean and extremum radiances for the pixels labeled "clear" from the first two steps are calculated over 5 and 30 day periods. Statistics are calculated for a 3x3 cell centered on the pixel of interest over the time period (i.e., 45 pixels are used for the 5 day period, and 270 for the 30 day period; this cell hereafter referred to as the "compositing cell"). Note that this cell size is acceptable from the point of view of spatial autocorrelation ranges, as discussed in section 4.1. The number and mean of clear pixels only is recorded as well as the maximum temperature and minimum albedo for all pixels (regardless of label).

Clear sky radiance map. The clear sky radiances for the pixels which are not variable are determined for 5 day periods. Variability here is determined by a series of statistical tests, after which the clear sky value may be the mean value over the period, the extremum (minimum visible and maximum thermal), or undetermined.

Bispectral threshold. The data are compared to the clear sky values modified by a threshold amount. Those that differ in either the thermal or visible channels by more than the threshold amount are labeled as cloud.

A thoroughly-tested version of the algorithm for low- and mid-latitudes has been applied to polar data by Rossow (1987). The algorithm misses approximately 20% of the cloud (Rossow, 1987, personal communication). Problems cited include: "real" cloud amount is high which forces the algorithm to use more extreme values for clear sky radiances; no distinction is made between snow-covered and snow-free land, or sea ice and open water in setting thresholds; thresholds were not tuned to the low radiances encountered in polar regions; and no adjustments were made for solar zenith angle.

2.3 Modifications

The algorithm has been adjusted here in order to deal with these problems. The adjustments are:

1. Data are corrected for solar zenith angle.
2. Subregion sizes in step 1, classification, are set to 100 km on a side for all surface types as suggested by the coherence and autocorrelation analyses.
3. A number of modifications take account of the variety and temporal variability of surface types.
4. 30-day periods are not used in the compositing step. Only five-day means and extremum are considered.
5. Missing values in the clear sky maps are filled based on neighboring pixels and the autocorrelation functions.
6. AVHRR channels 1 and 3 are also employed for the detection of low cloud over ice and snow.
7. If the statistical tests during compositing fail, the clear sky value determined for a given location is assigned a value based on its spatial neighbors or class characteristic value.
8. The bispectral threshold step uses channel 3 for ice and snow rather than channel 1.

Some of these modifications require further explanation.

2.3.1 Spatial and Temporal Variation Tests

In the spatial variation test of the initial classification, pixels are labeled "cloudy" if they are colder than the warmest pixel in the subregion by the amounts specified in Table 1. Subregions sizes suggested by Rossow (1987)

for this spatial variation test are "about 100 km over land and 300 km over ocean". However, five different surface types (snow-covered and snow-free land, ocean, sea ice, coast) may occur within subregions of these suggested sizes, $(300\ km)^2$ areas of open water are rare, and the autocorrelation analysis presented previously would suggest that these sizes are too large. Therefore, subregions of size $(100\ km)^2$ (20 x 20 pixel cells) were used regardless of the underlying surface type.

Table 1

Spatial and temporal thresholds for the three AVHRR channels and each surface type. Values for land and ocean are from original ISCCP specifications; those for other surfaces were derived experimentally. Values are in Kelvin.

	LAND	OCEAN	ICE	SNOW
Spatial	6.5	3.5	3.5	4.0
Temporal				
Cloud	8.0	3.5	5.0	7.0
Clear				
Ch. 1	4.4	1.4	8.8	3.8
Ch. 3	5.0	4.5	4.5	4.5
Ch. 4	2.5	1.1	2.0	2.0

In the temporal variation test of the initial classification, where pixel temperatures are compared to the day before and after, if a pixel is much colder than either day by the amount in Table 1, then that pixel is labeled "cloud". If the temperature is the same as either the preceding or following day (by the amount also shown in Table 1, 'Clear') then the pixel is labeled "clear". Otherwise, it is labeled "undecided". Obvious problems occur when warm, low

clouds move into or out of a region where the surface temperature is within the "clear" range of the cloud. These cloudy pixels will consequently be labeled clear in this step, and were probably labeled "undecided" in the spatial variation step because of their relatively high temperature. In this case, they will ultimately be labeled clear and used in the compositing step to determine clear sky radiances. Since these IR tests fail to label these pixels correctly, channel 1 and channel 3 data were also used in the temporal variation test.

Two other spatial/temporal approaches to the initial classification were tested. Rather than comparing each day to the day before and after, the warmest pixel in the seven days of data for each location was found. However, the warmest pixel in the period was often low cloud, and if the pixel under examination was also low cloud, even tests incorporating channels 1 and 3 may find little variability and the pixel will be mislabeled as clear. A test of each pixel against the warmest in the subregion for any day in the period (and of the same surface type) was also performed. Even if a further requirement that the warmest also have the lowest albedo is included, periods with persistent cloud cover often identify low cloud as the warmest and darkest.

2.3.2 Compositing

In the algorithm specifications (Rossow, 1987) the compositing step is to use 5-day means if there are enough clear pixels, or 30-day means or extremum otherwise. In the polar regions, surface characteristics may be too variable for 30-day values to be reasonable, particularly in the mid to late summer when snow may occur and sea ice moves and changes in concentration. Therefore, it is assumed that pixels within a reasonably small spatial area on the same day and of the same surface type will be no less similar than the same pixel up to

thirty days later.

If the statistical tests during compositing fail, the clear sky value for a given location is assigned a value based on its spatial neighbors or class characteristic value. The neighborhood of pixels with the same surface type is searched and the first clear value found for a pixel of the same surface type is used. The maximum radius is determined by an autocorrelation function (up to a radius of 12 pixels). If no value is found within this radius, the clear sky value assigned is based on the class characteristic values: the channel 1 value assigned is the mean for the surface type minus one standard deviation, the channel 3 value is the class mean, and the channel 4 value is the mean plus one standard deviation. These channel 1 and 4 values correspond to extrema. Channel 3 is more difficult as the relationship between brightness temperature for cloud and surfaces changes with particle size and physical temperature.

2.3.3 Surface Types

Surface types are determined with a land/permanent ice cap mask, SMMR data, and SMMR-derived sea ice concentration. The determination of land/not land is made with the land mask. If the pixel is land, then a SMMR test is applied to determine if the land is snow-free or snow-covered. Snow-covered land exhibits a higher brightness temperature at 18 GHz than at 37 GHz (e.g., Schweiger, 1987). The vertical polarization is less variable than the horizontal for land (unless wet). Hence, if the pixel is land and the 18 GHz vertical polarization brightness temperature is higher than in the 37 GHz vertical channel, it is labeled snow. This relationship may not hold over an ice cap, so a mask for permanent ice cap (e.g., Greenland and Novaya Zemlya) is included. Ice cap is labeled snow because of similar albedos. Problems with

this method also occur in coastal areas where this relationship may be observed even without the presence of snow. Therefore a coastal zone extending approximately 20 km from the coastline both inland and seaward is defined. Finally, if the pixel is not land and if the sea ice concentration is less than 15%, the pixel is labeled water, otherwise it is sea ice.

A problem occurs when the warmest pixel in a subregion is of one surface type and the pixel under examination is of another. For example, if the warmest pixel is clear sky over land and the pixel under examination is clear sky over sea ice, it is likely that the temperature difference will exceed the threshold and the sea ice pixel will be labeled cloud. Therefore, a "warmest" pixel for each surface type within a subregion is determined. Similarly, only those pixels in the compositing cell that have the same surface type as the center pixel are counted in the determination of mean and extremum values.

The basic ISCCP algorithm assumes a constant surface type over the five-day period. In most cases, this assumption is valid. However, snow melt in the spring and snowfall in late summer are particular problems for this algorithm. Perhaps equally likely is ice advection into or out of a region. In both cases, emissivities of the surface change, thereby affecting the response in the thermal channels. Additionally, albedos change dramatically so that those portions of the algorithm which incorporate visible data will be affected the most. The problem lies in the determination of the clear sky composite maps for the visible and thermal channels. If, for example, sea ice moved into a region on the last day of the period, the average albedo making up the clear sky value would be significantly affected. This is illustrated in Figure 3, which consists of cloud mapped with the AVHRR data and surface types identified using SMMR (18 and 37 GHz) and SMMR-derived sea ice concentrations. Cloud cover and

surface types are shown for the first day of the seven-day analysis period. Surface types are again shown for the sixth day. The change in ice extent to the northeast and south of Novaya Zemlya, and the associated change in surface albedo and temperature that will in turn affect the spectral responses of overlying cloud, illustrate problems that will limit the applicability of the ISCCP algorithm in areas with snow and ice cover. If the algorithm detected this problem and instead chose an extremum (minimum albedo) for the composite value from the first four days, this last day pixel would be labeled "cloud" in the final bispectral threshold test. Therefore, pixels in which the surface changes during the period are flagged, and do not receive a clear sky value in the compositing step. A possible solution is to determine clear sky values for each surface type at a location, using data from a 30-day period.

2.3.4 Statistical Tests

In order to provide a "population" against which to test compositing cell statistics, class characteristic values (i.e., mean and standard deviation) for each surface type are computed and updated with each region analyzed. These values are initially set to those determined for the previous 5-day period, or from training areas if no previous data are available. Those clear sky composite mean values which pass the statistical tests are incorporated into the new class characteristic values.

The statistical tests are designed to determine the likelihood that the clear pixels in each compositing cell are in fact all clear. This is done by examining the mean, standard deviation, and extremum of the cell. Channel 3 was used in addition to channel 4 for snow and ice surfaces. The procedure followed here is first to check the number of clear pixels in the compositing cell

(maximum 45). The cutoff value for too few pixels is a sample size, n, such that we could predict the population mean from the sample mean to within one population standard deviation (arbitrary), σ, at the 1-α confidence level, i.e.,

$$n = \left[\frac{z_{\alpha/2}\,\sigma}{E} \right]^2$$

where $E = \sigma$ is the maximum error. At a level of significance, α, of 0.01, this criterion requires that sample statistics and further tests be based on at least six clear pixels. If n is less than six then the maximum thermal and minimum visible values are used in the clear sky composite, assuming that the probability of them coming from the appropriate populations is greater than the specified α-level.

If, on the other hand, the number of clear pixels is sufficient, the probability that the minimum thermal and maximum visible values come from the population is tested. If the probability of obtaining either a smaller thermal or larger visible value is less than alpha, cloud contamination is assumed and the opposite extrema are used as the clear sky composite values. Otherwise, a t-test is perfomed on the means of the composite cell and the class characteristic values where the null hypothesis is that the means of the respective populations are equal (or the difference is 0). The calculated test value is

$$t = \frac{\bar{x}_1 - \bar{x}_2}{\sigma_E}$$

where σ_E is the standard error of the estimate:

$$\sigma_E = \left[\frac{(n_1-1)s^2_1 + (n_2-1)s^2_2}{n_1 + n_2 - 2}\right]^{1/2} \left[\frac{1}{n_1} + \frac{1}{n_2}\right]^{1/2}$$

if the population variances are equal or

$$\sigma_E = \left[\frac{s^2_1}{n_1} + \frac{s^2_2}{n_2}\right]^{1/2}$$

otherwise, with degrees of freedom of n_1+n_2-2 in both cases. The equality of variances is tested with the F statistic, which is the ratio of the two sample variances, s^2_i. If the null hypothesis in both tests is not rejected, then the mean values are used as the clear sky composite. Otherwise, extrema are used.

2.3.5 Thresholds and the Distribution of Cloud/Surface Differences

The final thresholding step utilizes AVHRR channels 1, 3, and 4. Channel 3 is used only if the surface is sea ice or snow/ice cap, and is intended to detect low cloud. Of course, middle and high clouds will be detected over any surface with thermal data alone. Thresholds for this step are given in Table 2. These thresholds are relatively large so that the algorithm yields a rather conservative estimate of cloud fraction.

Table 2

Final Thresholds for the three AVHRR channels and each surface type.

Channel	LAND	OCEAN	ICE	SNOW
1	6.0	3.5	6.0	4.0
2	6.0	6.0	5.0	5.0
3	8.0	3.0	4.0	4.0

In this final cloud detection step, a pixel is labeled cloud if it varies from the clear sky value by more than the threshold in **either** channel. The importance of this disjunction is illustrated in Figure 4 where the differences between cloudy pixel radiances and the radiance of the underlying surface - taken to be the clear sky composite value - are plotted for each channel. The data are based on samples taken from a number of regions containing a variety of surface types and cloud distributions. Zero differences are found along the line in each plot. Of particular interest are the points near this line, representing optically thin clouds over ice or snow in channel 1, and low (possibly inversion) clouds in the channel 4 plot. Those near the zero difference line in the channel 3 plot are not clouds with channel 4 temperatures similar to the surface, as these tend to exhibit higher brightness temperatures than the underlying surface in this channel. A few examples of this situation appear as points above the line. These clouds have been found to have temperatures and albedos similar to underlying snow and ice surfaces, particularly near the North Pole and over Greenland. Of course, a further problem is that the difference between channel 3 temperatures for this cloud type would be less for locations where the extremum thermal value is used in the

composite rather than the mean.

2.4 Synthetic Data Sets

In order to test the sensitivity of the components of the ISCCP algorithm, a control data set with known characteristics was needed. This section describes the development of a synthetic data set which consists of seven days of AVHRR data (channels 1, 3, 4), three days of SMMR data (every other day; 18 and 37 GHz vertical polarization) and sea ice concentration, and a land mask. Data sets were created as both a simple geometric representation of clouds and surfaces with no internal spectral variation and a free-form model with spectral variation controlled by one or more theoretical probability distributions.

The procedure followed was to first generate the surface and cloud type maps for each day of the seven day period. Surface types are snow-covered and snow-free land, open water, and sea ice. Cloud layers are classified as low, middle, and high, where levels are defined by AVHRR channel 4 temperatures as follows: low cloud - > 265 K, middle cloud - 245-265 K, high cloud - < 245 K. These class maps can be manually produced using an image analysis system, where "objects" may take on any shape and size, or they can be generated automatically. Both methods were tested and, for the purposes of algorithm validation, produced similar images. Due to the relative ease of automatically generating the synthetic images, this method was followed.

When the class maps are automatically generated, the minimum and maximum allowable sizes of surface objects for the first day, and cloud objects for each day are specified. An object is generated whose x,y dimensions are randomly chosen (uniform random number generator, URNG) within the restricted range, and the class of the object is randomly assigned (URNG).

Regions were then filled with data for each AVHRR and SMMR channel and for sea ice concentration. This filling was done with empirically-derived statistics. Data were based on class characteristic values (means and standard deviations) computed from training areas. Data values for each pixel in each channel were produced using a random number generator, the most important being one that produces normally distributed random numbers (NRNG). Each artificially-generated element of class j is a vector, v_j, of d features:

$$v_j = \mu_j + \Omega A_j$$

where μ_j is the class mean vector of length d, Ω is a vector of random deviations for each feature selected from the multivariate Gaussian distribution of deviations, A_j is the lower triangular matrix decomposed from the d x d class covariance matrix, Σ_j (which is symmetric and positive definite), such that

$$A_j A_j^T = \Sigma_j$$

The values from the Gaussian random number generator have a zero mean and unit variance and are constrained to be in the range of -3 to +3 which include approximately 99% of the data in a normally distributed population. Random number generators that produce values following uniform, negative exponential, and lognormal distributions are also possible.

The surface map for the first day and cloud maps for all days were created with the above procedure. The surface maps for the third and fifth days, however, were modified versions of the first day. Snow and ice pixels were allowed to melt into land and water, respectively; ice pixels may advance into open water areas and snow may fall on land. The evolution was designed such that approximately 68% of the decisions resulted in an unchanged local area and

32% of the decisions resulted in either an advance or a retreat. Note that this adjustment produces non-rectangular surface regions.

Synthetic data sets provide a model of the world observed through AVHRR and SMMR sensors. The model can be developed as simple geometrical shapes with no internal spatial and temporal variation or as free-form shapes with fuzzy edges (possibly fractal), texture, variable cloud properties and emissivities, spatially or temporally autocorrelated spectral properties, and so on. An intermediate level of complexity was chosen here, where the main concern was spatial and temporal variability of clouds and surfaces.

2.5 Testing and Algorithm Comparison

Four versions of the ISCCP algorithms are compared. The basic algorithm (abbreviated O-ISCCP) developed for low latitude summer conditions[1] recognizes only two surface types: land and water. No SMMR or sea ice concentration data are employed. Spatial/temporal tests in the initial classification step are thermal only (AVHRR channel 4). A bispectral threshold test (channels 1 and 4) is used as the final classification. This version with a thermal-only threshold test was also used to simulate winter applications (OT-ISCCP). The algorithm with modifications decribed above was the third version tested (M-ISCCP). The primary differences are in the recognition of multiple and changing surface types, and the inclusion of AVHRR channel 3 in the spatial/temporal tests, statistical tests, and in the threshold tests. Finally, the modified algorithm was used with a channel 3 and 4 difference threshold to identify clear pixels

[1]This is not the identical algorithm applied by William Rossow at NASA, but rather a separate implementation which follows the same basic steps.

rather than the spatial/temporal tests (E-ISCCP). With this method, if the difference between the two channels is less than 4.5 K, the pixel is considered clear. If the difference is between 4.5 and 6.0 K, it is labeled "undecided", otherwise it is labeled as cloud. This method is based in part upon the work of Oleson and Grassl (1985).

Four regions from the AVHRR imagery and four regions from the synthetic data sets are used as test data. Each region is 50 x 50 pixels or $(250\ km)^2$ and differs in surface and cloud types and proportions. The synthetic data set image contains surface areas with 250 to 500 km as the minimum dimension ("objects" are rectangular). Cloud sizes and distributions changed from day to day, with the minimum dimension ranging from 20 to 300 km. Surface proportions changed in both data sets by up to 20%. These changes were due to sea ice movement and melting. The surface/cloud types and proportions for each region are given in Table 3.

Cloud fractions computed by each algorithm for each region and day are given in Tables 4 and 5. Also given in the table are the number of clear pixels used in the compositing step for each region and version. The actual cloud amount is shown for synthetic data sets, determined by counting the number of pixels in the region assigned to a cloud category. A manual interpretation was done using the image analysis system with all AVHRR, SMMR, and SMMR-derived data sets available. However, this value is only an approximation, and results from the algorithms may be more accurate. When cloud amounts are small to moderate, the manual interpretation generally overestimates cloud fraction. When cloud amounts are high, the manually interpreted cloud fraction is more accurate, but may slightly underestimate cloud fraction.

Table 3

Percentages of surface and cloud types within the eight test regions. Cloud data are given for the middle five days of the seven day analysis period. Cloud categories are low, middle, and high. Surface types are land (L), water (W), ice (I), and snow/ice cap (S).

Region:day	Synthetic Data Low, Middle, High(%)	AVHRR Data Low, Middle, High(%)
1: 2	4, 28, 39	0, 0, 3
3	24, 43, 6	72, 18, 0
4	47, 41, 11	14, 0, 7
5	6, 0, 81	10, 20, 16
6	58, 8, 33	52, 10, 33
Surface:	W(100)	I(100)
2: 2	29, 0, 58	12, 12, 75
3	21, 42, 17	13, 30, 53
4	30, 12, 16	27, 41, 30
5	0, 17, 78	18, 43, 38
6	55, 7, 37	18, 80, 0
Surface:	L(35), W(65)	W(100)
3: 2	0, 33, 0	10, 17, 53
3	24, 20, 24	17, 33, 10
4	59, 20, 21	10, 45, 25
5	0, 0,100	0, 20, 3
6	20, 25, 16	15, 40, 20
Surface:	W(24), S(76)	L(80), W(12), I(8)
4: 2	0, 52, 0	5, 10, 82
3	31, 14, 54	35, 30, 30
4	12, 0, 28	71, 10, 0
5	10, 20, 51	28, 25, 7
6	48, 18, 17	17, 50, 23
Surface:	L(22), W(12), I(66)	W(45), S(27), I(22), L(6)

Table 4

"Actual" cloud fraction for synthetic data and cloud fraction computed by the four versions of the ISCCP algorithm. Values are for each of the middle five days of an analysis period. Cloud fraction computed by the bispectral threshold step is first given; cloud fraction determined after the initial classification is given in parentheses. The number of clear pixels in the compositing step is also shown. See text for version symbols.

		Algorithm			
Region:day	Actual	O-ISCCP	OT-ISCCP	M-ISCCP	E-ISCCP
1: 2	71	76 (76)	76 (76)	78 (75)	71 (75)
3	73	80 (84)	80 (84)	75 (71)	73 (73)
4	99	100 (68)	98 (68)	100 (68)	100 (100)
5	87	90 (93)	90 (93)	90 (90)	88 (86)
6	99	100 (85)	98 (85)	100 (69)	100 (100)
# clear:	--	643	643	125	1581
2: 2	87	93 (100)	92 (100)	94 (85)	90 (88)
3	80	97 (100)	97 (100)	82 (82)	80 (79)
4	58	83 (100)	80 (100)	77 (75)	66 (59)
5	95	100 (100)	100 (100)	95 (92)	95 (95)
6	99	100 (100)	98 (100)	100 (66)	100 (100)
# clear:	--	219	219	71	1691
3: 2	33	82 (56)	78 (56)	83 (46)	79 (34)
3	68	94 (76)	91 (76)	94 (65)	93 (68)
4	100	100 (67)	94 (67)	100 (70)	100 (100)
5	100	100 (98)	100 (98)	100 (96)	100 (100)
6	61	96 (97)	90 (97)	97 (87)	96 (59)
# clear:	--	415	415	425	2326
4: 2	52	90 (67)	76 (67)	58 (62)	76 (57)
3	99	99 (100)	98 (100)	99 (100)	98 (100)
4	40	79 (83)	66 (83)	54 (53)	65 (44)
5	81	98 (98)	95 (98)	81 (93)	93 (88)
6	83	96 (96)	88 (96)	92 (82)	92 (90)
# clear:	--	420	420	32	2105

Table 5

Cloud fraction for actual data as computed by manual interpretation and four versions of the ISCCP algorithm. Abbreviations are the same as Table 5.2.

		Algorithm			
Region:day	Manual	O-ISCCP	OT-ISCCP	M-ISCCP	E-ISCCP
1: 2	3	56 (5)	2 (5)	1 (6)	2 (12)
3	90	99 (50)	78 (50)	79 (39)	93 (100)
4	21	70 (6)	12 (6)	10 (6)	17 (85)
5	46	90 (44)	65 (44)	55 (42)	56 (97)
6	95	99 (61)	89 (61)	85 (57)	98 (100)
# clear:	--	2404	2404	2264	2327
2: 2	99	99 (100)	99 (100)	100 (98)	99 (99)
3	96	97 (100)	81 (100)	98 (88)	98 (99)
4	98	94 (68)	75 (68)	96 (58)	94 (78)
5	99	100 (100)	99 (100)	100 (99)	100 (100)
6	98	92 (100)	73 (100)	98 (83)	95 (87)
# clear:	--	159	159	9	1000
3: 2	80	83 (78)	75 (78)	85 (72)	83 (90)
3	60	62 (54)	55 (54)	61 (53)	57 (64)
4	80	83 (87)	73 (87)	80 (80)	80 (85)
5	23	31 (27)	18 (27)	29 (23)	23 (27)
6	75	77 (79)	72 (79)	77 (76)	75 (86)
# clear:	--	1509	1509	972	2129
4: 2	97	100 (100)	99 (99)	100 (100)	100 (100)
3	97	99 (65)	63 (65)	98 (58)	97 (58)
4	81	95 (52)	46 (52)	85 (44)	79 (82)
5	60	76 (48)	51 (48)	75 (51)	65 (63)
6	90	95 (79)	80 (79)	92 (85)	91 (91)
# clear:	--	1031	1031	362	1594

Haze is difficult to detect with the image analysis system. While this condition is detected by the difference between channels 3 and 4, it is still difficult to observe in a color composite because the temperature and albedo are both very near those of the underlying surface. Visual detection requires an examination of actual brightness temperatures and albedos, and a comparison with the same area under other conditions. Of course, this is exactly what the ISCCP algorithm is designed to do.

All versions of the algorithm performed best over land and water. Snow and ice remain the problem areas although the modified versions performed best under these conditions. When cloud amounts are high (more than 80%), all versions compute cloud fraction to within approximately 5%. When cloud amounts were low, the modified versions are more accurate, although cloud fraction is often too high. In the actual data, this is at least in part due to errors in the manual interpretation, as described above. In the synthetic data, this is probably due to the fact that clear sky areas are filled with values in the range of the mean plus or minus three standard deviations (following a Gaussian probability function), so that extreme values may be beyond threshold cutoffs and will consequently be labeled as cloud.

The basic versions often overestimate cloud amount by up to 20%. This is particularly true over ice where, in the bispectral threshold test, the threshold for water is used. This albedo threshold is too small to account for variation in sea ice albedos, and consequently many clear pixels are mistaken for cloud. This can be seen for region 1, day 2 of the actual data. Similar observations were made by Rossow (1987). A related situation is that the basic version often makes an accurate assessment of cloud fraction, but for the wrong reason. Day 3 of the same region and data set had over 70% of the cloud cover

as very thin cloud, possibly haze. Channels 1 and 4 alone cannot normally detect this condition, yet the threshold determined cloud amount for O-ISCCP is similar to the manually-determined amount. Here again, albedo contributions from the thin cloud are insignificant, so that the algorithm is calling "cloud" by the threshold step what it sees in channel 1 as sea ice. The snow and ice data sets used in the modified versions solve these problems by providing appropriate thresholds.

An examination of the fraction of the region labeled "undecided" in the inital classification revealed that this value was smaller for the modified versions and that the difference between their initially classified cloud fraction and the threshold-determined cloud fraction was also smaller. This indicates that these versions are generally more stable. However, the number of clear pixels used in the compositing step was quite small for M-ISCCP, indicating that the three-channel spatial/temporal tests are perhaps too restrictive, as noted also in the previous chapter. Additionally, there were a few sequences where most pixels in a region were clear every other day, so that the temporal variation tests would never label these pixels as clear.

The channel 3 minus 4 initial classification method proved to be problematic under certain cloud conditions. There were many occurrences of optically thick clouds with similar brightness temperatures in both channels which seemed not to be limited to a narrow range of temperatures. These conditions were initially classified as clear, and may or may not have been reclassified by the statistical tests. Therefore, the spatial/temporal classification tests - although not without problems - are more reliable for the actual data. Olesen and Grassl (1985) used AVHRR channel 5 in conjunction with the channel 3,4 difference, where the surface temperature was assumed to be

higher than that of the cloud. The two-dimensional histogram was then examined and partitioned into surface and cloud layers. This scheme would often fail with polar data since the surface temperatures are similar (and in winter usually lower) than low cloud temperatures due to ground-based inversions.

Winter conditions in the Arctic can be particularly difficult to deal with algorithmically for two major reasons: strong surface inversions are the norm and no visible data are available. It is not unusual to find that the coldest object in the image is the surface. The data for study area 3 (January 6-12, 1984) is no exception, where almost all cloud layers are warmer than the surface. Even over open water cold air advected from the adjacent ice creates weak lapse rates and/or inversions. Surface temperatures over land were 225-235 K, ocean (open and thin ice) in the southern portion of the image was 260-275 K, sea ice was 231-235 K, and clouds ranged from 215 to 258 K.

To apply the ISCCP algorithm, additional modifications were necessary. The spatial variation test - where the warmest pixel in a subregion is considered clear - is certainly not valid. Therefore, this step was eliminated and the temporal variation test was used alone for the initial classification. The assumption that clouds are colder than the surface is found again in the final threshold step. This was modified so that a difference from the clear sky composite value in either direction signals a cloudy pixel. Finally, temperatures within the broadly-defined surface classes varied considerably across the image, in particular for snow/ice cap over Greenland (elevation change) and open water from the Norwegian Sea northward to Spitsbergen. Class characteristic values were no longer reliable, so statistical tests for cloud contamination were based only on the range of the extremum.

3.0 Summary

Modifications to the basic ISCCP algorithm for cloud mapping over polar surfaces are proposed. The modified algorithm (M-ISCCP) is expected to yield an improvement in accuracy (estimated to be 5-10%) in computed cloud amount over the original, thermal-only version, depending on surface type and cloud proportions. This claim is for Arctic summers, from 60°N latitude to the pole, and is based on the tests results presented above, proportions of surface types over the Arctic, and average cloud amounts (see Section 1.2.4 and related references). All versions perform best over snow-free land and open water, so that improvement will be greater than this figure over snow, ice cap, and sea ice and less over open water and snow-free land. The most useful modification to the basic algorithm seems to be the ability to deal with additional surface types (i.e., sea ice and snow/ice cap) which allows a more appropriate choice of thresholds.

Unfortunately, extracting, calibrating, and registering three or more AVHRR channels for seven days, two SMMR channels for each of three days, calculating sea ice concentration for three days, and developing a land/ice cap mask is not a trivial undertaking, so that this procedure is cost-effective only in areas where the more basic methods fail; i.e., over snow and ice. Previous studies (e.g. Rossow, 1987) have used only orbital AVHRR visible and thermal data.

Persistent cloud cover and the small temperature difference between low clouds and water, ice, and snow remain the most difficult problems to solve given the basic structure of the ISCCP algorithm. To reduce the number of misclassifications resulting from these situations, channels 1 and 3 were incorporated. Unfortunately, channel 1 and the reflected component of channel

3 are not available for wintertime data. However, d'Entremont (1986) and Olesen and Grassl (1985) have shown that the addition of channel 3 improves the detection of low clouds and fogs at night, and also detects thin cirrus more confidently than any single-window infrared data, so that improvement could be expected with its use. The difference between channels 3 and 4 aids in the detection of optically thin cloud.

The initial classification step is the most difficult part of the algorithm to refine due to its sensitivity to changes in thresholds. Error will propagate from this point, so it is important that all pixels labeled "clear" in this step actually are clear, but it is also important to obtain as many clear pixels as possible. The spatial/temporal tests are generally accurate, but fail in the case where a pixel is cloudy every other day. Using the simple channel 3 and 4 difference test for clear sky pixels was found to ease the computational burden and increase accuracy, but it fails for some middle-and low-level optically thick cloud decks. Under persistent cloud cover, the 5-day compositing period may not be long enough to obtain an adequate sample of clear pixels. An examination of winter polar data undertaken here indicates that thermal-only spectral features are helpful, but alone are not sufficient unless examined over time.

In summary, the best method of cloud detection includes first an accurate identification of surface types and changes. This allows thresholds to be set appropriately. Next the temporal variability of pixel radiances must be examined, using channel 4 and the reflected component of AVHRR channel 3 during summer, and the difference between channels 3 and 4 in conjunction with channels 4 or 5 for winter analyses. Temporal changes are most important in winter, as surfaces may be colder than cloud layers and spectral information alone is

inadequate. Compositing over a 5-day period, using 30-day values where necessary, provides the clear sky information for the final bispectral thresholding of the daily data. Channels 1, 3 (reflected), and 4 may be used with summer data, and channels 3 (or 3-4) and 4 (or 5) should be used for winter analyses.

Finally, the lack of 'ground truth' makes testing and validation difficult. Synthetic data sets provide a model of the world as observed through AVHRR and SMMR sensors. The model can be developed as simple geometrical shapes with no internal spatial and temporal variation or as free-form shapes with fuzzy edges (possibly fractal), texture, variable cloud properties and emissivities, autocorrelated spectral properties, and so on. The degree to which they model reality tests our understanding of the theoretical and empirical nature of the systems and how well we can couple these approaches into a precise description of the world. An intermediate level of complexity was chosen here; the main concern being spatial and temporal variability of clouds and surfaces. They provide a data set with known characteristics that allows performance to be quantified.

4.0 Work Planned for the Last Six Months

In the last six months of the second (and last) project year, work will continue on the ISCCP algorithm testing and modification for use in the polar regions. As described in this report, a number of problems with the application of this algorithm remain unsolved. In addition, a broader cloud analysis procedure will be developed from the modified ISCCP algorithm, where clouds are first detected and parameterized on the pixel scale, and cloud patterns and types are then be determined on a regional, $(250\ km)^2$ scale. The ultimate goal

is to automate further and objectify the process of developing polar cloud climatologies for the purpose of monitoring climate change. Some background work on spring and summer Arctic cloud types has been done through a combination of manual and digital techniques by Kukla (1984), Robinson et al. (1986), Barry et al. (1987), and McGuffie et al. (1988).

References

Barry, R.G. and R.G. Crane, 1985. Synoptic cloud climatology of the Arctic Ocean. **Abstract Digest, Science Review of the NASA Climate Research Program**, Science and Technology Corp., Hampton, VA: 51.

Barry, R.G. A. Henderson-Sellers, and K.P. Shine, 1984. Climate sensitivity and the marginal cryosphere, in Climate Processes and Climate Sensitivity, J. Hansen and T. Takahashi (eds.), Geophys. Monog. 29, Amer. Geophys. Union, Washington, DC, pp. 221-337.

Barry, R.G., R.G. Crane, A. Schweiger, and J. Newell, 1987. Arctic cloudiness in spring from satellite imagery, **J. Climatol.**, 7, 423-451.

Crane, R.G. and R.G. Barry, 1984. The influence of clouds on climate with a focus on high latitude interactions, **J. Climatol.**, 4, 71-93.

Garand, L., 1988. Automated recognition of oceanic cloud patterns. Part I: methodology and application to cloud climatology, **J. Climate**, 1, 20-39.

Kukla, G.J., 1984. Variation of Arctic cloud cover during summer 1979, Part 1, Technical Report LDGO-84-2, Lamont-Doherty Geological Observatory of Columbia University.

Olesen, F. and H. Grassl, 1985. Cloud detection and classification over oceans at night with NOAA-7, **Int. J. Remote Sensing**, 6 (8), 1435-1444.

Raschke, E., 1987. "Report of the ISCCP workshop on cloud algorithms in the polar regons," National Institute for Polar Research, WCP-131, WMO/TD-No. 170, Tokyo, Japan, 19-21 August 1986.

Rossow, W.B., 1987. "Application of ISCCP cloud algorithm to satellite observations of the polar regions," in Raschke, E., 1987. "Report of the ISCCP workshop on cloud algorithms in the polar regons," National Institute for Polar Research, WCP-131, WMO/TD-No. 170, Tokyo, Japan, 19-21 August 1986.

Rossow, W.B., 1987. "Preliminary documentation for ISCCP C1 data set", Pilot Climate Data System, Goddard Institue for Space Studies, NASA.

Rossow, W.B., F. Mosher, E. Kinsella, A. Arking, M. Desbois, E. Harrison, P. Minnis, E. Ruprecht, G. Seze, C. Simmer, and E. mith, 1985. "ISCCP cloud algorithm intercomparison," J. Clim. Appl. Meteor., 24, 877-903.

Schweiger, A., 1987. Retrieval of snow cover parameters using passive radiometry in the Federal Republic of Germany, Unpublished Master's thesis, Department of Geography, University of Colorado, Boulder.

Serreze, M.S. and R.G. Barry, 1988. Synoptic activity in the Arctic Basin, 1979-85, **J. Climate** (in press).

Vowinckel, E., 1962. Cloud amount and type over the Arctic, Publications in

Meteorology, No. 51, Montreal: Arctic Meteorology Research Group, McGill University, p. 27.

Vowinckel, E., and S. Orvig, 1970. The climate of the North Polar Basin, in Climates of the Polar Regions, S. Orvig, ed., World Survey of Climatology, 14, Elsevier, Amsterdam, 370 pp.

WMO, 1987. Report of the ISCCP workshop on cloud algorithms in the polar regons, World Climate Research Programme, WCP-131, WMO/TD-No. 170, Tokyo, Japan, 19-21 August 1986.

Publications Supported in Whole or Part by NAG-5-898

Barry, R.G., Crane, R.G., Newell, J., and Schweiger, A., 1988. "Arctic cloudiness in spring from satellite imagery. A response," **J. Climatol.**, 8, 539-540.

Crane, R.G. and Barry, R.G., 1988. "Comparison of the MSL synoptic pressure patterns of the Arctic as observed and simulated by the GISS General Circulation Model," **Meteor. Atmos. Physics**, in press.

Key, J., Maslanik, J.A., and Barry, R.G. "Cloud classification using a fuzzy sets algorithm: a polar example," **Int. J. Remote Sensing**, in press.

Key, J.R., 1988. "Cloud analysis in the Arctic with combined AVHRR and SMMR data," unpublished Ph.D. dissertation, University of Colorado, Boulder, 180 pp.

Maslanik, J.A., Key, J.R., and Barry, R.G. "Merging AVHRR and SMMR data sea ice and cloud analysis," **Int. J. Remote Sensing**, in press.

Maslanik, J.A., Barry, R.G., and Crane, R.G., 1987. "Approaches to the interpretation of cloud cover in the polar regions," (abstract). Clouds in Climate II. (A WCRP Workshop on Modeling and Observations, Columbia, MD). WCRP, NASA, NSF, NOAA, and DOE, p. 169.

McGuffie, K., Barry, R.G., Newell, J., Schweiger, A., and Robinson, D., 1988. "Intercomparison of satellite-derived cloud analyses for the Arctic Ocean in spring and summer," **Int. J. Remote Sensing**, 9 (3), 467-477.

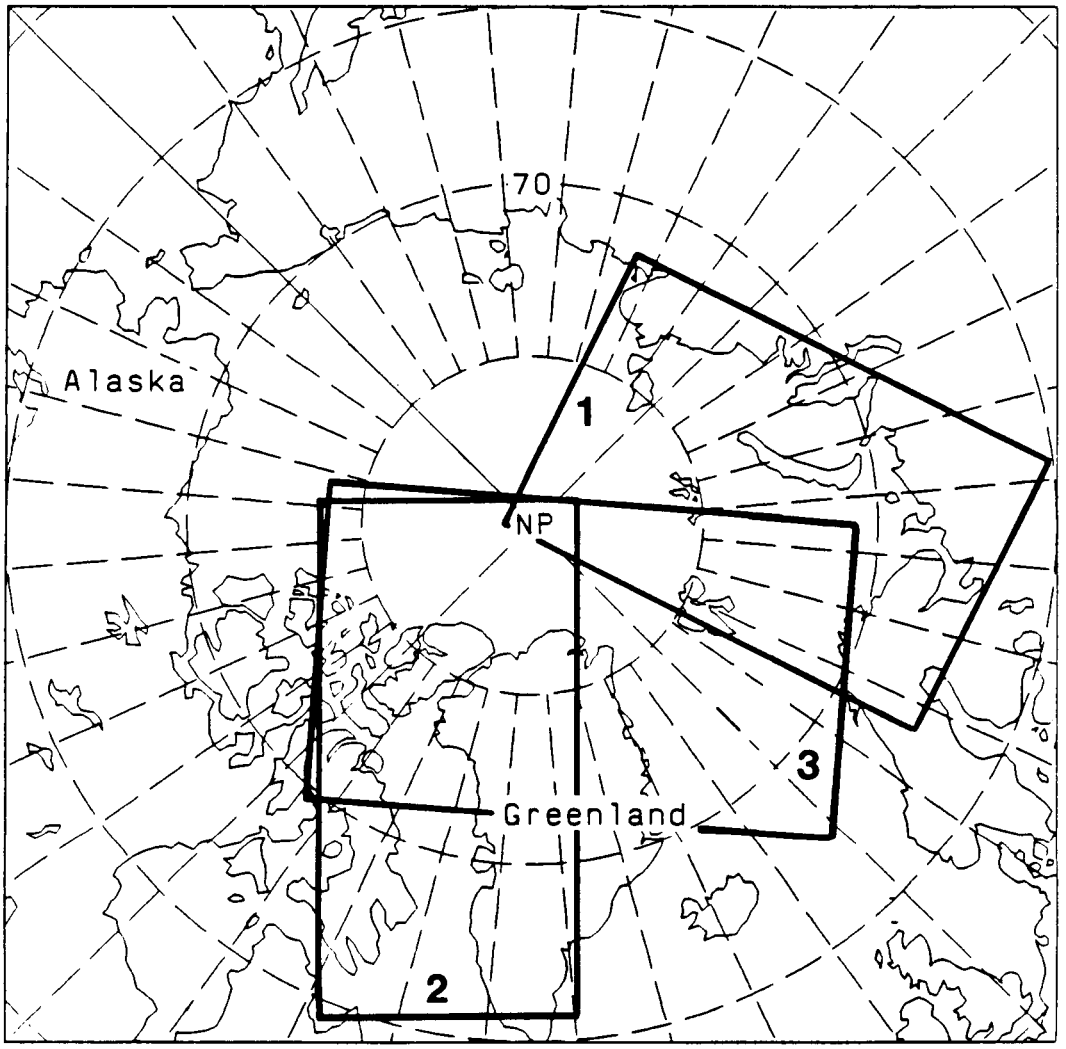

Fig. 1. The three study areas within the Arctic, one centered on the Kara and Barents Sea and the other two covering much of the Canadian Archipelago and northern Greenland.

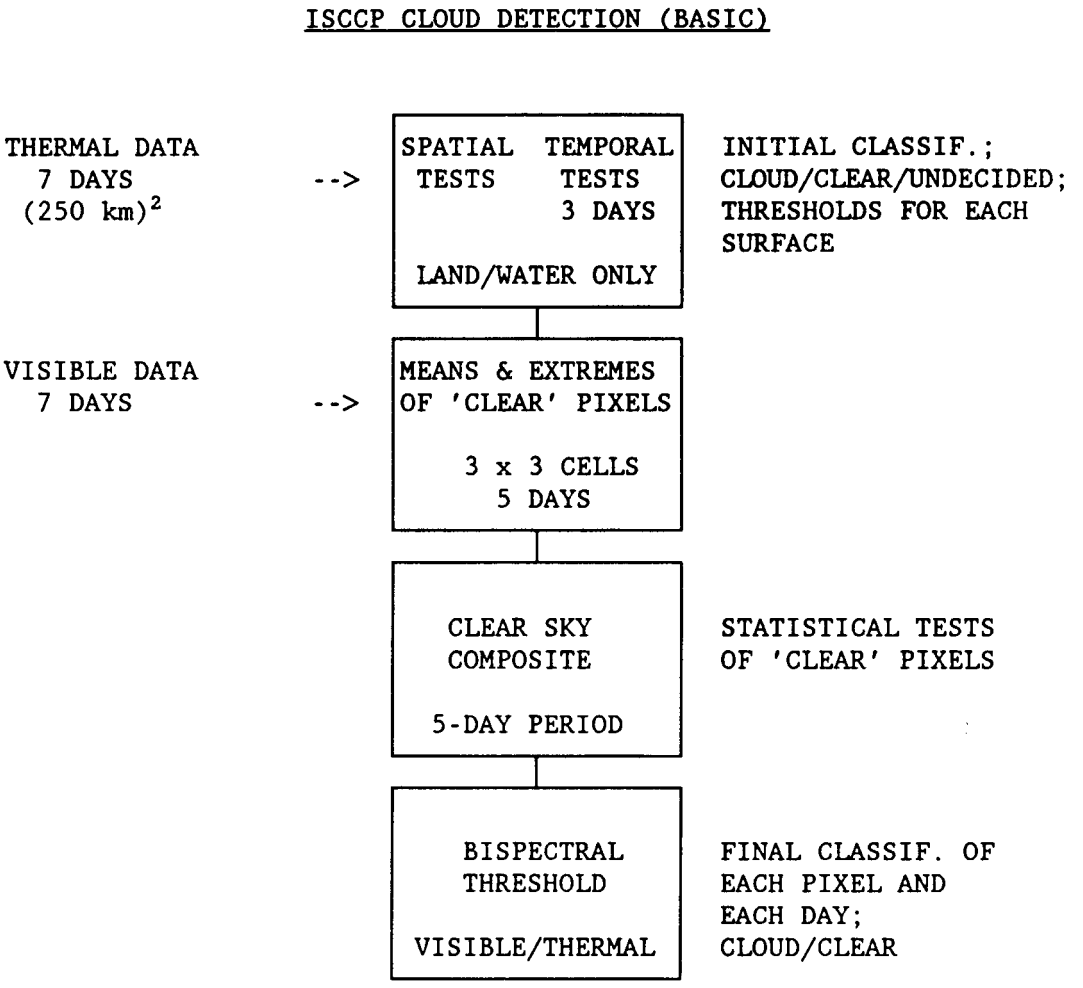

Fig. 2. Flow chart of the basic ISCCP algorithm. Input are shown on the left; additional details are given on the right.

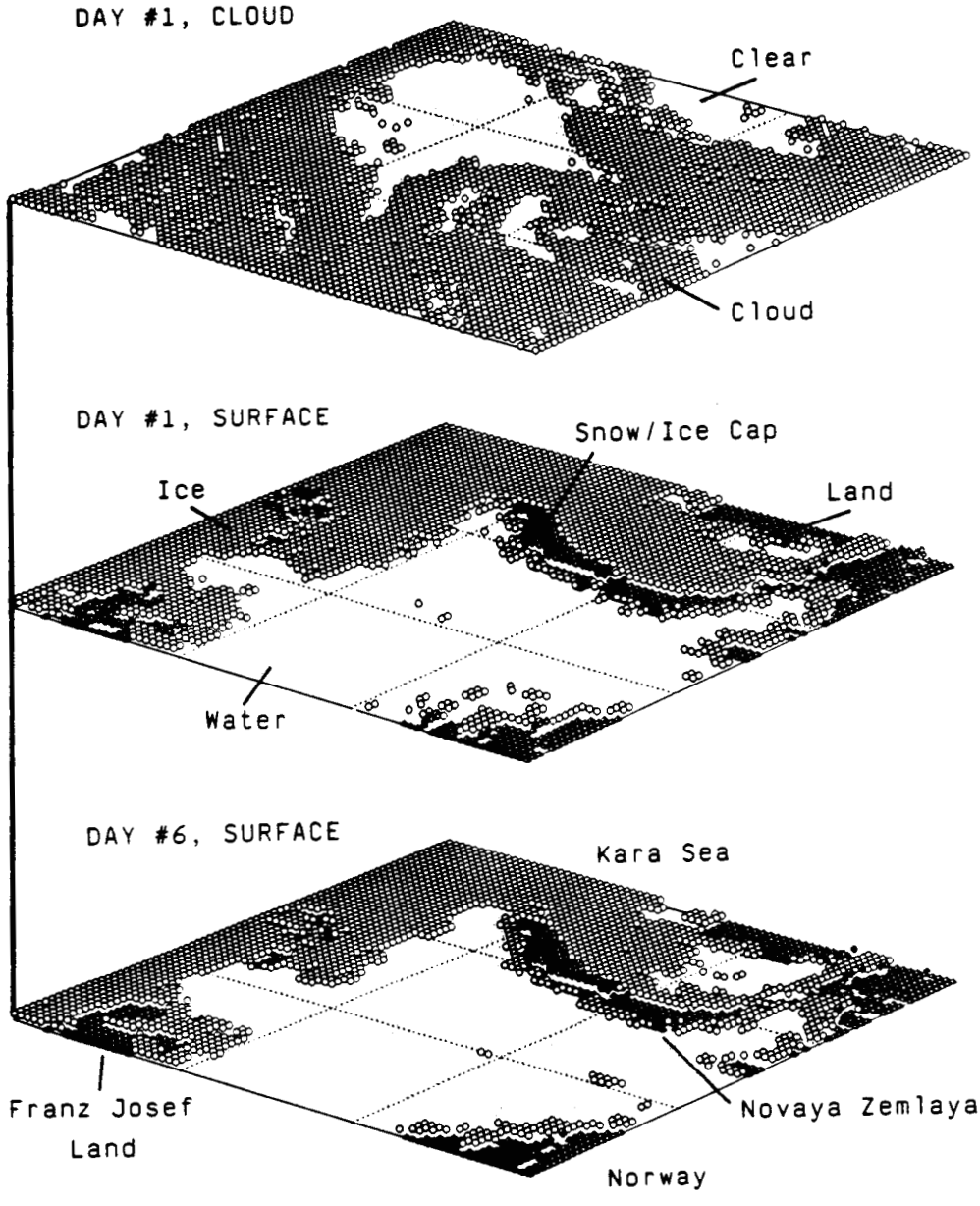

Fig. 3. Cloud cover and surface types for a single day and surface types for the same area five days later. Area covered is $(1500\ km)^2$. The combined AVHRR/SMMR data set provides for the mapping of cloud over varying surfaces, as shown here for changing ice extent northeast and south of Novaya Zemlya.

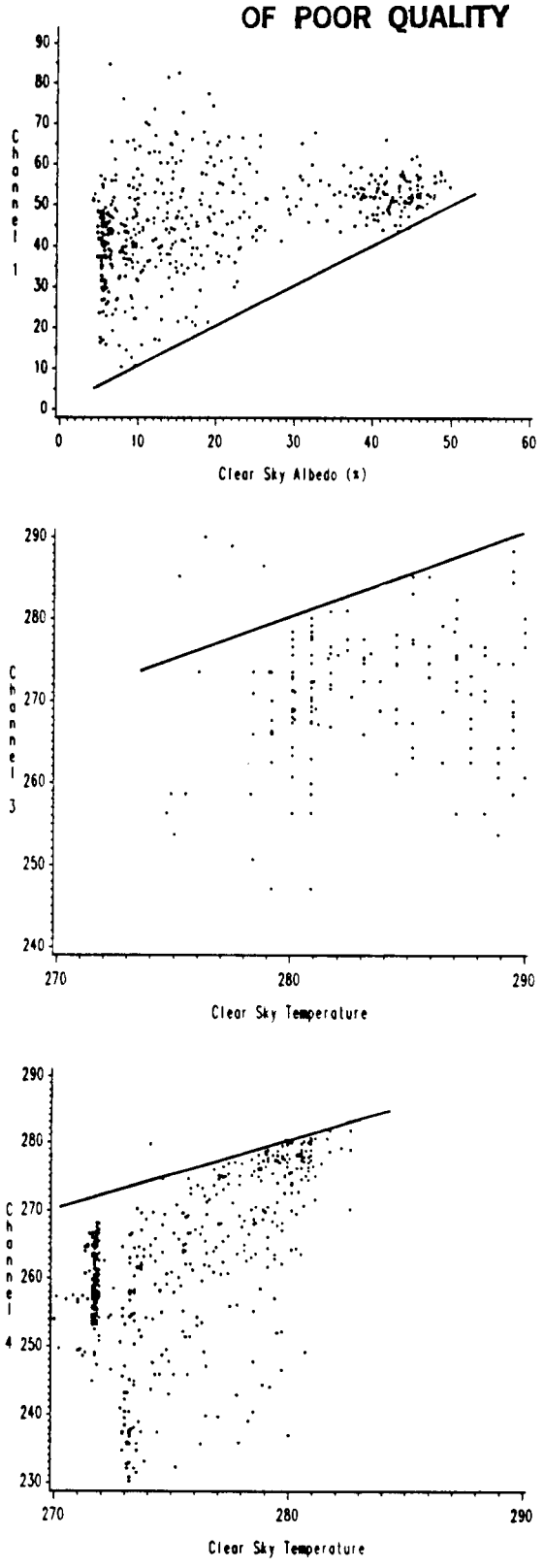

Fig. 4. Clear sky composite value (horizontal axis) vs. cloudy pixel radiance for those pixels classified as cloud in channels 1, 3, and 4.